Chap 6 Green function theory

Ming-Che Chang

Department of Physics, National Taiwan Normal University, Taipei, Taiwan

(Dated: January 3, 2018)

I. INTRODUCTION

We start with the Green function for systems at *zero* temperature. This is first developed systematically by F. Dyson in late 40's, in the context of QED. The Green function for systems at *finite* temperature is introduced in the next chapter.

A. Definition

In the Heisenberg picture,

$$a_\alpha^\dagger(t) = e^{iHt/\hbar} a_\alpha^\dagger e^{-iHt/\hbar}. \tag{1}$$

The one-particle **Green function** is defined as,

$$G_{\alpha\beta}(t,t') = -i\langle\Psi_0|Ta_\alpha(t)a_\beta^\dagger(t')|\Psi_0\rangle, \tag{2}$$

where $|\Psi_0\rangle$ is the exact manybody ground state, and T is the **time-ordering operator**,

$$Ta_\alpha(t)a_\beta^\dagger(t') \equiv \begin{cases} a_\alpha(t)a_\beta^\dagger(t') \text{ if } t > t', \\ -a_\beta^\dagger(t')a_\alpha(t) \text{ if } t < t'. \end{cases} \tag{3}$$

That is,

$$\begin{aligned} G_{\alpha\beta}(t,t') = & - i\theta(t-t')\langle\Psi_0|a_\alpha(t)a_\beta^\dagger(t')|\Psi_0\rangle \\ & + i\theta(t'-t)\langle\Psi_0|a_\beta^\dagger(t')a_\alpha(t)|\Psi_0\rangle. \end{aligned} \tag{4}$$

We can also define the **retarded Green function**,

$$\begin{aligned} G^R_{\alpha\beta}(t,t') = & - i\theta(t-t')\langle\Psi_0|a_\alpha(t)a_\beta^\dagger(t')|\Psi_0\rangle \\ & - i\theta(t-t')\langle\Psi_0|a_\beta^\dagger(t')a_\alpha(t)|\Psi_0\rangle. \end{aligned} \tag{5}$$

The original Green function is easier for calculation, but the retarded Green function is closer to experimental observables.

Given an one-body operator,

$$A = \sum_{\alpha\beta} A^{(1)}_{\alpha\beta} a_\alpha^\dagger a_\beta, \tag{6}$$

its expectation value can be written in Green function,

$$\langle\Psi_0|A(t)|\Psi_0\rangle = -i\sum_{\alpha\beta} A^{(1)}_{\alpha\beta} G_{\beta\alpha}(t,t^+). \tag{7}$$

The arguments t, t' in the formulation above can be extended to $(\mathbf{r},t),(\mathbf{r}',t')$, and

$$\langle\Psi_0|A(\mathbf{r},t)|\Psi_0\rangle = -i\sum_{\alpha\beta} A^{(1)}_{\alpha\beta} G_{\beta\alpha}(\mathbf{r},t,\mathbf{r},t^+). \tag{8}$$

For example, for the particle density,

$$\rho(\mathbf{r},t) = \psi^\dagger(\mathbf{r},t)\psi(\mathbf{r},t), \tag{9}$$

we have

$$\langle\Psi_0|\rho(\mathbf{r},t)|\Psi_0\rangle = -iG(\mathbf{r},t,\mathbf{r},t^+). \tag{10}$$

B. Non-interacting system

Consider a non-interacting Hamiltonian,

$$H_0 = \sum_\alpha \varepsilon_\alpha a_\alpha^\dagger a_\alpha. \tag{11}$$

Since

$$i\hbar\dot{a}_\alpha = [a_\alpha, H_0] = \varepsilon_\alpha a_\alpha, \tag{12}$$

we have

$$a_\alpha(t) = e^{-i\omega_\alpha t} a_\alpha(0), \quad \omega_\alpha \equiv \varepsilon_\alpha/\hbar, \tag{13}$$

and

$$\langle\Phi_0|a_\alpha(t)a_\beta^\dagger(t')|\Phi_0\rangle = e^{-i\omega_\alpha t + i\omega_\beta t'}\delta_{\alpha\beta}(1-n_\alpha), \tag{14}$$

in which $|\Phi_0\rangle$ is the non-interacting manybody ground state.

As a result,

$$\begin{aligned} & G_{\alpha\beta}(t,t') \\ = \; & e^{-i\omega_\alpha(t-t')}\delta_{\alpha\beta}[-i\theta(t-t')(1-n_\alpha) + i\theta(t'-t)n_\alpha], \end{aligned} \tag{15}$$

which is diagonal in α,β, and depends only on $t-t'$. Similarly,

$$G^R_{\alpha\beta}(t,t') = -ie^{-i\omega_\alpha(t-t')}\delta_{\alpha\beta}\theta(t-t'). \tag{16}$$

Also,

$$\begin{aligned} G_{\alpha\beta}(\omega) &= \int_{-\infty}^{\infty} dt e^{i\omega t} G_{\alpha\beta}(t) \\ &= -i\delta_{\alpha\beta}\int_0^\infty dt e^{i(\omega-\omega_\alpha)t}e^{-\eta t}(1-n_\alpha) \\ &\quad + i\delta_{\alpha\beta}\int_{-\infty}^0 dt e^{i(\omega-\omega_\alpha)t}e^{+\eta t}n_\alpha \\ &= \delta_{\alpha\beta}\underbrace{\frac{1-n_\alpha}{\omega-\omega_\alpha+i\eta}}_{\text{from empty states}} + \delta_{\alpha\beta}\underbrace{\frac{n_\alpha}{\omega-\omega_\alpha-i\eta}}_{\text{from filled states}} \end{aligned} \tag{17}$$

The factors $e^{\mp\eta t}(\eta = 0^+)$ are inserted to ensure that the exponentials could converge at $t = \pm\infty$.

Similarly, for the retarded Green function,

$$G^R_{\alpha\beta}(\omega) = \delta_{\alpha\beta}\frac{1-n_\alpha}{\omega-\omega_\alpha+i\eta} + \delta_{\alpha\beta}\frac{n_\alpha}{\omega-\omega_\alpha+i\eta} \quad (18)$$

$$= \delta_{\alpha\beta}\frac{1}{\omega-\omega_\alpha+i\eta}. \quad (19)$$

Note that the factors $\pm i\eta$ play a crucial role here.

For a free electron gas, $\alpha = (\mathbf{k}, s)$, and $(G_\alpha \equiv G_{\alpha\alpha})$,

$$G_{ks}(\omega) = \frac{1-n_k}{\omega-\omega_k+i\eta} + \frac{n_k}{\omega-\omega_k-i\eta}. \quad (20)$$

For the ground state at $T = 0$, the first term vanishes for $\varepsilon_k < \mu$, while the second term vanishes for $\varepsilon_k > \mu$.

C. Interacting system, Lehmann representation

Consider *interacting* systems and focus on diagonal Green function,

$$G_\alpha(t,t') = -i\theta(t-t')\langle\Psi_0|a_\alpha(t)1a^\dagger_\alpha(t')|\Psi_0\rangle + i\theta(t'-t)\langle\Psi_0|a^\dagger_\alpha(t')1a_\alpha(t)|\Psi_0\rangle. \quad (21)$$

Insert complete sets to the locations of 1 above,

$$1 = \sum_n |\Psi^\wedge_n\rangle\langle\Psi^\wedge_n| = \sum_n |\Psi^\vee_n\rangle\langle\Psi^\vee_n|, \quad (22)$$

where $|\Psi^\wedge_n\rangle$ and $|\Psi^\vee_n\rangle$ are the *exact* energy eigenstates for $(N+1)$-particles and $(N-1)$-particles. With the relation,

$$\langle\Psi_0|a_\alpha(t)|\Psi^\wedge_n\rangle = \langle\Psi_0|e^{iHt/\hbar}a_\alpha e^{-iHt/\hbar}|\Psi^\wedge_n\rangle = e^{-i\omega^\wedge_{n0}t}\langle\Psi_0|a_\alpha|\Psi^\wedge_n\rangle, \quad (23)$$

$$\hbar\omega^\wedge_{n0} \equiv E^{N+1}_n - E^N_0,$$

we have,

$$\begin{aligned} & G_\alpha(t,t') \quad (24)\\ =& -i\theta(t-t')\sum_n e^{-i\omega^\wedge_{n0}t}e^{i\omega^\wedge_{n0}t'}\langle\Psi_0|a_\alpha|\Psi^\wedge_n\rangle\langle\Psi^\wedge_n|a^\dagger_\alpha|\Psi_0\rangle \\ &+ i\theta(t'-t)\sum_n e^{+i\omega^\vee_{n0}t}e^{-i\omega^\vee_{n0}t'}\langle\Psi_0|a^\dagger_\alpha|\Psi^\vee_n\rangle\langle\Psi^\vee_n|a_\alpha|\Psi_0\rangle \\ =& -i\theta(t-t')\sum_n e^{-i\omega^\wedge_{n0}(t-t')}|\langle\Psi^\wedge_n|a^\dagger_\alpha|\Psi_0\rangle|^2 \\ &+ i\theta(t'-t)\sum_n e^{+i\omega^\vee_{n0}(t-t')}|\langle\Psi^\vee_n|a_\alpha|\Psi_0\rangle|^2 = G_\alpha(t-t'). \end{aligned}$$

Also, one can show that,

$$G_\alpha(\omega) = \int_{-\infty}^{\infty} dt e^{i\omega t}G_\alpha(t) \quad (25)$$

$$= \sum_n\left(\frac{|\langle\Psi^\wedge_n|a^\dagger_\alpha|\Psi_0\rangle|^2}{\omega-\omega^\wedge_{n0}+i\eta} + \frac{|\langle\Psi^\vee_n|a_\alpha|\Psi_0\rangle|^2}{\omega+\omega^\vee_{n0}-i\eta}\right).$$

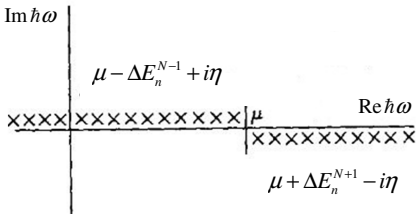

FIG. 1 Singularities of the Green function in complex $\hbar\omega$-plane.

This is called the **spectral representation**, or the **Lehmann representation** of the Green function. Note that,

$$\hbar\omega^\wedge_{n0} = E^{N+1}_n - E^N_0 = \underbrace{E^{N+1}_n - E^{N+1}_0}_{=\Delta E^{N+1}_n} + \underbrace{E^{N+1}_0 - E^N_0}_{=\mu(N)} > \mu. \quad (26)$$

The pole of the second term is at

$$-\hbar\omega^\vee_{n0} = -(E^{N-1}_n - E^N_0) = -\underbrace{(E^{N-1}_n - E^{N-1}_0)}_{=\Delta E^{N-1}_n} + \underbrace{E^N_0 - E^{N-1}_0}_{=\mu(N-1)} < \mu. \quad (27)$$

See Fig. 1 for the location of poles. We have assumed that $N \gg 1$, so that $\mu(N \pm 1) \simeq \mu(N)$.

For the retarded Green function, we have

$$G^R_\alpha(\omega) = \int d\omega' \frac{A_\alpha(\omega')}{\omega-\omega'+i\eta}, \quad (28)$$

where

$$A_\alpha(\omega') \equiv \sum_n |\langle\Psi^\wedge_n|a^\dagger_\alpha|\Psi_0\rangle|^2\delta(\omega'-\omega^\wedge_{n0}) + \sum_n |\langle\Psi^\vee_n|a_\alpha|\Psi_0\rangle|^2\delta(\omega'+\omega^\vee_{n0}) > 0. \quad (29)$$

It gives the energy resolution of a particle in state-α, and is called the **spectral function**. It can be shown that,

$$\int_{-\infty}^{\infty} d\omega A_\alpha(\omega) = \langle\Psi_0|a_\alpha a^\dagger_\alpha|\Psi_0\rangle + \langle\Psi_0|a^\dagger_\alpha a_\alpha|\Psi_0\rangle = 1. \quad (30)$$

The spectral function can be measured by photo-emission or electron tunnelling. See p. 442 of Ref. 1 for more details.

Conversely, the spectral function can be written in retarded Green function,

$$A_\alpha(\omega) = -\frac{1}{\pi}\mathrm{Im}\ G^R_\alpha(\omega). \quad (31)$$

Local density of states (LDOS) is the spectral function with spatial resolution,

$$A(\mathbf{r},\omega) = -\frac{1}{\pi}\text{Im } G^R(\mathbf{r},\mathbf{r},\omega) \quad (32)$$

$$= \sum_n |\langle\Psi_n^\wedge|\psi^\dagger(\mathbf{r})|\Psi_0\rangle|^2\delta(\omega'-\omega_{n0}^\wedge) + \sum_n |\langle\Psi_n^\vee|\psi(\mathbf{r})|\Psi_0\rangle|^2\delta(\omega'+\omega_{n0}^\vee). \quad (33)$$

The LDOS can be probed by STM.

For non-interacting systems, from Eq. (19), one has

$$A_\alpha(\omega) = \delta(\omega-\omega_\alpha). \quad (34)$$

If the state-α is not steady, but decays with time due to interaction, then

$$G_\alpha^R(t) = -i\theta(t)e^{-i\omega_\alpha t}e^{-t/\tau}. \quad (35)$$

As a result,

$$G_\alpha^R(\omega) = \frac{1}{\omega-\omega_\alpha+\frac{i}{\tau}}, \quad (36)$$

and the spectral function is a broadened delta function (Lorentzian distribution),

$$A_\alpha(\omega) = \frac{1}{\pi}\frac{1/\tau}{(\omega-\omega_\alpha)^2+(1/\tau)^2} \equiv \delta_\tau(\omega-\omega_\alpha). \quad (37)$$

II. EQUATION OF MOTION

Start from

$$G_{\alpha\beta}(x,x') = -i\theta(t-t')\langle\psi_\alpha(x)\psi_\beta^\dagger(x')\rangle_0 + i\theta(t'-t)\langle\psi_\beta^\dagger(x')\psi_\alpha(x)\rangle_0,$$

we have,

$$i\partial_t G_{\alpha\beta}(x,x') = +\delta(t-t')\langle\psi_\alpha(x)\psi_\beta^\dagger(x')\rangle_0 + \delta(t'-t)\langle\psi_\beta^\dagger(x')\psi_\alpha(x)\rangle_0 - i\theta(t-t')\langle i\partial_t\psi_\alpha(x)\psi_\beta^\dagger(x')\rangle_0 + i\theta(t'-t)\langle\psi_\beta^\dagger(x')i\partial_t\psi_\alpha(x)\rangle_0. \quad (38)$$

For interacting fermions,

$$H = \int dv\psi_\gamma^\dagger(\mathbf{r},t)H_0\psi_\gamma(\mathbf{r},t) \quad (39)$$

$$+ \frac{1}{2}\int dv_1dv_2\psi_\gamma^\dagger(\mathbf{r}_1)\psi_\delta^\dagger(\mathbf{r}_2)V(\mathbf{r}_1-\mathbf{r}_2)\psi_\delta(\mathbf{r}_2)\psi_\gamma(\mathbf{r}_1),$$

in which every field operator has the same time t. Let $x=(\mathbf{r},t)$, then the **equation of motion** (EOM) for field operator is ($\hbar\equiv 1$),

$$i\frac{\partial\psi_\alpha(x)}{\partial t} = [\psi_\alpha, H] = H_0\psi_\alpha(x) + \int d^4x_1\psi_\gamma^\dagger(x_1)V_s(x-x_1)\psi_\gamma(x_1)\psi_\alpha(x),$$

in which

$$V_s(x-x_1) \equiv V(\mathbf{r}-\mathbf{r}_1)\delta(t-t_1). \quad (40)$$

It is a static instantaneous potential. Therefore,

$$\begin{aligned} & i\partial_t G_{\alpha\beta}(x,x') \\ =\ & \delta_{\alpha\beta}\delta(x-x') + H_0G_{\alpha\beta}(x,x') \\ -\ & i\theta(t-t')\int d^4x_1V_s(x-x_1)\langle\psi_\gamma^\dagger(x_1)\psi_\gamma(x_1)\psi_\alpha(x)\psi_\beta^\dagger(x')\rangle_0 \\ +\ & i\theta(t'-t)\int d^4x_1V_s(x-x_1)\langle\psi_\beta^\dagger(x')\psi_\gamma^\dagger(x_1)\psi_\gamma(x_1)\psi_\alpha(x)\rangle_0 \\ =\ & \delta_{\alpha\beta}\delta(x-x') + H_0G_{\alpha\beta}(x,x') \\ -\ & i\int d^4x_1V_s(x-x_1)\langle T\psi_\alpha(x)\psi_\gamma(x_1)\psi_\gamma^\dagger(x_1^+)\psi_\beta^\dagger(x')\rangle_0, \end{aligned} \quad (41)$$

where $x_1=(\mathbf{r}_1,t_1)$, $x_1^+\equiv(\mathbf{r}_1,t_1+0^+)$. Note that inside the time-ordering product, a minus sign pops up whenever we exchange two fermion operators.

Define the **two-particle Green function** as,

$$\begin{aligned} & G_{\alpha\beta\gamma\delta}(x_1,x_2,x_3,x_4) \\ =\ & (-i)^2\langle\Psi_0|T\psi_\alpha(x_1)\psi_\beta(x_2)\psi_\gamma^\dagger(x_3)\psi_\delta^\dagger(x_4)|\Psi_0\rangle, \end{aligned} \quad (42)$$

then

$$\begin{aligned} & \left(i\frac{\partial}{\partial t}-H_0\right)G_{\alpha\beta}(x,x') \\ +\ & i\int d^4x_1V_s(x-x_1)G_{\alpha\gamma\gamma\beta}(x,x_1,x_1^+,x') \\ =\ & \delta_{\alpha\beta}\delta(x-x'). \end{aligned} \quad (43)$$

The EOM for two-particle Green function would in turn be related to four-particle Green function ... etc. To solve the EOM, approximation is required by writing the two-particle Green function approximately in terms of one-particle Green functions.

The expectation value of a two-body operator can be written in terms of two-particle Green function. Given an operator,

$$A = \frac{1}{2}\sum_{\alpha\alpha'\beta'\beta}A^{(2)}_{\alpha\alpha'\beta'\beta}a_\alpha^\dagger a_{\alpha'}^\dagger a_{\beta'}a_\beta, \quad (44)$$

using the Green function, its expectation value can be written as,

$$\langle\Psi_0|A(t)|\Psi_0\rangle = -\frac{1}{2}\sum_{\alpha\alpha'\beta\beta'}A^{(2)}_{\alpha\alpha'\beta'\beta}G_{\beta'\beta\alpha\alpha'}(t,t,t^+,t^+). \quad (45)$$

For example, for the interaction,

$$V = \frac{1}{2}\int dvdv'V^{(2)}_{\alpha\alpha'\beta'\beta}\psi_\alpha^\dagger(\mathbf{r})\psi_{\alpha'}^\dagger(\mathbf{r}')\psi_{\beta'}(\mathbf{r}')\psi_\beta(\mathbf{r}), \quad (46)$$

one has (p. 116 of Ref. 2)

$$\langle V\rangle = -\frac{1}{2}\int dvdv'V^{(2)}_{\alpha\alpha'\beta'\beta}G_{\beta'\beta\alpha\alpha'}(\mathbf{r}',0,\mathbf{r},0;\mathbf{r},0^+,\mathbf{r}',0^+). \quad (47)$$

III. PERTURBATION THEORY

One major problem in calculating the Green function is that $|\Psi_0\rangle$ is unknown, which is the manybody ground state of

$$H = H_0 + V. \tag{48}$$

Assuming H_0 is solvable, then one can treat V as a perturbation, and calculate the Green function using perturbation expansion.

A. Interaction picture

Recall that in the **Schrödinger picture**, the operators are fixed, and the states evolve with e^{-iHt}. In the **Heisenberg picture**, the states are fixed, while the operators evolve with e^{-iHt}. In the **interaction picture**, we let the operators evolve with H_0,

$$A_I(t) = e^{iH_0 t} A e^{-iH_0 t}, \tag{49}$$

and the states evolve as,

$$\begin{aligned} |\Psi_I(t)\rangle &= e^{iH_0 t}|\Psi_S(t)\rangle \\ &= e^{iH_0 t}U(t)|\Psi_S\rangle, \end{aligned} \tag{50}$$

with

$$i\partial_t U(t,t') = H(t)U(t,t'). \tag{51}$$

Therefore,

$$i\partial_t|\Psi_I(t)\rangle = V_I(t)|\Psi_I(t)\rangle, \tag{52}$$

$$\text{where } V_I(t) = e^{iH_0 t} V e^{-iH_0 t}. \tag{53}$$

If one writes

$$|\Psi_I(t)\rangle = U_I(t,t')|\Psi_I(t')\rangle, \tag{54}$$

then the evolution operator satisfies,

$$i\partial_t U_I(t,t') = V_I(t)U_I(t,t'). \tag{55}$$

Therefore,

$$\begin{aligned} U_I(t,t') &= 1 - i\int_{t'}^{t} dt_1 V_I(t_1)U_I(t_1,t') \\ &= 1 + (-i)\int_{t'}^{t} dt_1 V_I(t_1) \\ &+ (-i)^2 \int_{t'}^{t} dt_1 \int_{t'}^{t_1} dt_2 V_I(t_1)V_I(t_2) \\ &+ \cdots \end{aligned} \tag{56}$$

For the third term, we can write

$$\begin{aligned} &\int_{t'}^{t} dt_1 \int_{t'}^{t_1} dt_1 V_I(t_1)V_I(t_2) \\ &= \frac{1}{2}\int_{t'}^{t} dt_1 \int_{t'}^{t_1} dt_2 V_I(t_1)V_I(t_2) \quad (t \geq t_1 \geq t_2 \geq t') \\ &+ \frac{1}{2}\int_{t'}^{t} dt_2 \int_{t'}^{t_2} dt_1 V_I(t_2)V_I(t_1) \quad (t \geq t_2 \geq t_1 \geq t') \\ &= \frac{1}{2}\int_{t'}^{t} dt_1 \int_{t'}^{t} dt_2 \theta(t_1 - t_2)V_I(t_1)V_I(t_2) \\ &+ \frac{1}{2}\int_{t'}^{t} dt_2 \int_{t'}^{t} dt_1 \theta(t_2 - t_1)V_I(t_2)V_I(t_1) \\ &= \frac{1}{2}\int_{t'}^{t} dt_1 \int_{t'}^{t} dt_2 T[V_I(t_1)V_I(t_2)]. \end{aligned} \tag{57}$$

This can be applied to high-order terms. For example, for the next order, there are 3! ways to arrange the order of t_1, t_2, t_3. Thus,

$$\begin{aligned} U_I(t,t') &= \sum_{n=0}^{\infty} \frac{1}{n!}\int_{t'}^{t} dt_1 \cdots dt_n T\left[V_I(t_1)\cdots V_I(t_n)\right] \\ &\equiv T\, e^{-i\int_{t'}^{t} dt'' V_I(t'')}. \end{aligned} \tag{58}$$

So far, no approximation has been used.

B. Gell-Mann and Low theorem

Since we have no idea what $|\Psi_0\rangle$ is, we need to rely on *non-interacting* manybody ground state $|\Phi_0\rangle$ to calculate the matrix elements. This can be done using the trick of adiabatic switch-on,

$$V_I(t) \to V_I(t)e^{-\epsilon|t|}. \tag{59}$$

That is, the interaction is turned on and off adiabatically. As a result,

$$\underbrace{|\Psi_{0I}\rangle}_{\text{interacting G.S.}} = U_I(0,-\infty) \underbrace{|\Phi_0\rangle}_{\text{non-int G.S.}} \tag{60}$$

$$\equiv U_I(0,-\infty)|-\infty\rangle. \tag{61}$$

Also,

$$|\Psi_{0I}\rangle = U_I(0,\infty)|\infty\rangle. \tag{62}$$

If the ground state (assumed to be non-degenerate) remains gapped from excited states, then after the evolution, we are back to the original ground state,

$$|\infty\rangle = e^{i\delta}|-\infty\rangle. \tag{63}$$

However, if the energy gap closes during the evolution, then the system may undergo a quantum phase transition. This brings a qualitative change to the ground state, and the perturbation approach fails.

Now,

$$\begin{aligned}
&\langle\Psi_0|A_H(t)|\Psi_0\rangle \\
&= \langle\Psi_{0I}(t)|A_I(t)|\Psi_{0I}(t)\rangle \\
&= \underbrace{\langle\infty|}_{e^{-i\delta}\langle-\infty|} U_I(\infty,t)A_I(t)U_I(t,-\infty)|-\infty\rangle \\
&= \frac{\langle-\infty|U_I(\infty,t)A_I(t)U_I(t,-\infty)|-\infty\rangle}{\langle-\infty|\infty\rangle} \\
&= \frac{\langle\Phi_0|T\left[e^{-i\int_{-\infty}^{\infty}dt'V_I(t')}A_I(t)\right]|\Phi_0\rangle}{\langle\Phi_0|T\ e^{-i\int_{-\infty}^{\infty}dt'V_I(t')}|\Phi_0\rangle}, \qquad (64)
\end{aligned}$$

in which $\langle-\infty|\infty\rangle = \langle-\infty|U_I(\infty,-\infty)|-\infty\rangle$. This equation is first derived by Gell-Mann and Low (1951). Similarly,

$$\begin{aligned}
&\langle\Psi_0|T[A_H(t_1)B_H(t_2)]|\Psi_0\rangle \\
&= \frac{\langle-\infty|U_I(\infty,t_1)A_I(t_1)U_I(t_1,t_2)B_I(t_2)U_I(t_2,-\infty)|-\infty\rangle}{\langle-\infty|\infty\rangle} \\
&= \frac{\langle\Phi_0|T\left[e^{-i\int_{-\infty}^{\infty}dt'V_I(t')}A_I(t_1)B_I(t_2)\right]|\Phi_0\rangle}{\langle\Phi_0|T\ e^{-i\int_{-\infty}^{\infty}dt'V_I(t')}|\Phi_0\rangle}. \qquad (65)
\end{aligned}$$

The first equality is for $t_1 > t_2$, but the case with $t_1 < t_2$ works the same way.

C. Wick theorem

According to the equation above,

$$\begin{aligned}
G_{\alpha\beta}(t,t') &= -i\langle\Psi_0|Ta_\alpha(t)a_\beta^\dagger(t')|\Psi_0\rangle \qquad (66)\\
&= -i\frac{\langle\Phi_0|T\left[e^{-i\int_{-\infty}^{\infty}dt''V_I(t'')}a_\alpha(t)a_\beta^\dagger(t')\right]|\Phi_0\rangle}{\langle\Phi_0|T\ e^{-i\int_{-\infty}^{\infty}dt'V_I(t')}|\Phi_0\rangle}.
\end{aligned}$$

Since V_I is quartic in $a_\alpha, a_\alpha^\dagger$, the Taylor expansion of $e^{-i\int dt'' V_I}$ would produce terms with many $a_\alpha, a_\alpha^\dagger$'s. We need a systematic method to calculate their matrix elements. The Wick theorem below is of great help to break down these higher order terms.

First, it helps to move annihilation operator a_α to the right, since it would annihilate the ground state $|\Phi_0\rangle$. Note: if $|\Phi_0\rangle$ is the Fermi sea, then
a_α is an annihilation operator if $\varepsilon_\alpha > \varepsilon_F$;
$a_\alpha^\dagger$ is an annihilation operator if $\varepsilon_\alpha < \varepsilon_F$.
This motivates us to define the **normal ordering**,

$$N(a_\alpha a_\beta^\dagger) \equiv -a_\beta^\dagger a_\alpha. \qquad (67)$$

Again there is a flip of sign whenever two fermion operators are exchanged.

Second, define the **contraction** of two creation or annihilation operators as,

$$\overbrace{AB} \equiv AB - N(AB). \qquad (68)$$

Since $N(AB) = AB$ or $-BA$, one has

$$\overbrace{AB} = 0 \text{ or } \{A,B\}, \qquad (69)$$

which is a c-number either way. Therefore,

$$\overbrace{AB} = \langle\Phi_0|\overbrace{AB}|\Phi_0\rangle = \langle\Phi_0|AB|\Phi_0\rangle. \qquad (70)$$

With time-ordering, we have

$$\begin{aligned}
\overbrace{AB} &= TA(t)B(t') - NA(t)B(t') \qquad (71)\\
&= \theta(t-t')A(t)B(t') - \theta(t'-t)B(t')A(t) - NA(t)B(t') \\
&= \begin{cases} -\theta(t'-t)\{A(t),B(t')\}, & \text{or } 0 \ \ (\text{for } t'>t), \\ +\theta(t-t')\{A(t),B(t')\}, & \text{or } 0 \ \ (\text{for } t>t'). \end{cases} \qquad (72)
\end{aligned}$$

in which $N(AB) = AB$, or $-BA$.

A and B are either a or $a^\dagger$, and in the interaction picture, $a_\alpha(t) = e^{iH_0t}a_\alpha e^{-iH_0t} = e^{-i\omega_\alpha t}a_\alpha$. Thus, the anti-commutators are numbers. For example, $\{a_\alpha,(t),a_\beta^\dagger(t')\} = e^{-i\omega_\alpha t + i\omega_\beta t'}\delta_{\alpha\beta}$. Therefore,

$$\overbrace{AB} = \langle\Phi_0|\overbrace{AB}|\Phi_0\rangle = \langle\Phi_0|TAB|\Phi_0\rangle. \qquad (73)$$

The fact that the anti-commutator between creation and annihilation operators is a delta function, instead of an operator, helps simplifying the contraction. This is crucial to the following analysis. It is not so for spin systems, for example, so that the Wick theorem is of limited use there.
Example 1:

$$\begin{aligned}
\overbrace{a_\alpha(t)a_\beta^\dagger(t')} &= \langle\Phi_0|Ta_\alpha(t)a_\beta^\dagger(t')|\Phi_0\rangle \\
&= iG^0_{\alpha\beta}(t,t'). \qquad (74)
\end{aligned}$$

That is, the contraction gives you a Green function. Also, it is not difficult to see that $\overbrace{a_\alpha(t)a_\beta(t')}$ and $\overbrace{a_\alpha^\dagger(t)a_\beta^\dagger(t')}$ are both zero.

Now we are ready to present the **Wick theorem** (1950):

$$\begin{aligned}
&T(ABC\cdots XYZ) \\
&= N(ABC\cdots XYZ) \\
&+ N(\overbrace{AB}\,C\cdots XYZ) + N(\overbrace{ABC}\cdots XYZ) + \cdots \\
&+ \text{2 pairs of contractions} \\
&+ \text{3 pairs of contractions} \\
&\cdots \\
&+ \text{all paired.} \qquad (75)
\end{aligned}$$

Be aware that to contract two operators, they need be brought together first, possibly producing a sign flip. It's not difficult to see that, after being sandwiched by $|\Phi_0\rangle$, all of the terms vanish, except the last one, which is a product of $G^0_{\alpha\beta}$'s (Example 1). The proof of the Wick

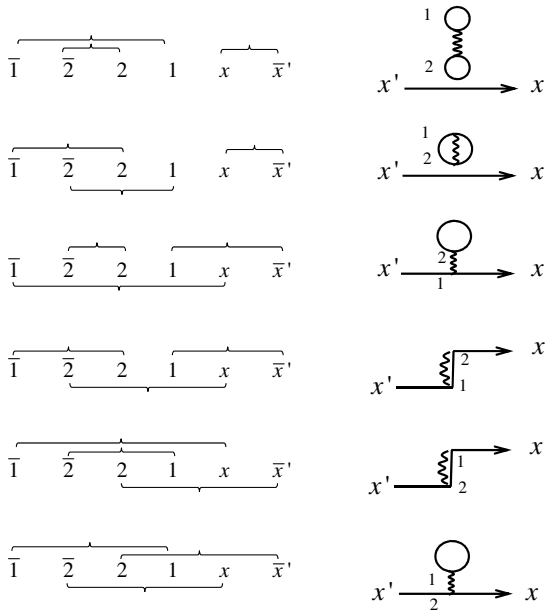

FIG. 2 Six ways to contract the field opeartors in Eq. (81), and their diagrams.

theorem can be found in Ref. 3, for example, and is not presented here.

Example 2: Recall that the contractions $\overbrace{a_\alpha a_\beta}$ and $\overbrace{a_\alpha^\dagger a_\beta^\dagger}$ are 0. Thus,

$$\begin{aligned} & T(a_\alpha^\dagger a_\beta^\dagger a_\gamma a_\delta) \\ = \; & N(a_\alpha^\dagger a_\beta^\dagger a_\gamma a_\delta) \\ - \; & N(a_\alpha^\dagger a_\gamma)\overbrace{a_\beta^\dagger a_\delta} + N(a_\alpha^\dagger a_\delta)\overbrace{a_\beta^\dagger a_\gamma} \\ - \; & \overbrace{a_\alpha^\dagger a_\gamma}\, N(a_\beta^\dagger a_\delta) + \overbrace{a_\alpha^\dagger a_\delta}\, N(a_\beta^\dagger a_\gamma) \\ - \; & \overbrace{a_\alpha^\dagger a_\gamma}\,\overbrace{a_\beta^\dagger a_\delta} + \overbrace{a_\alpha^\dagger a_\delta}\,\overbrace{a_\beta^\dagger a_\gamma}. \end{aligned} \tag{76}$$

IV. ONE-PARTICLE GREEN FUNCTION

We are now ready to calculate the Green function,

$$\begin{aligned} & G_{\alpha\beta}(\mathbf{r},t,\mathbf{r}',t') \\ = \; & -i\langle\Psi_0|T\psi_\alpha(\mathbf{r},t)\psi_\beta^\dagger(\mathbf{r}',t')|\Psi_0\rangle \\ = \; & -i\frac{\langle\Phi_0|T\left[e^{-i\int_{-\infty}^{\infty}dt''V_I(t'')}\psi_\alpha(x)\psi_\beta^\dagger(x')\right]|\Phi_0\rangle}{\langle\Phi_0|T\; e^{-i\int_{-\infty}^{\infty}dt'V_I(t')}|\Phi_0\rangle}, \end{aligned} \tag{77}$$

in which x, x' are 4-vectors, e.g., $x \equiv (t, \mathbf{r})$. All of the field operators are in the interaction representation. The

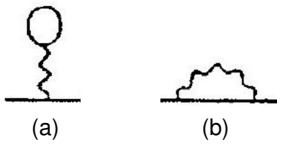

FIG. 3 Connected diagrams at the first order.

integral of the interaction can be written as,

$$\begin{aligned} & \int dt V_I(t) \\ = \; & \frac{1}{2}\int dt \int dv_1 dv_2 \psi_\gamma^\dagger(\mathbf{r}_1,t)\psi_\delta^\dagger(\mathbf{r}_2,t)V(\mathbf{r}_1-\mathbf{r}_2) \\ & \qquad \times\psi_\delta(\mathbf{r}_2,t)\psi_\gamma(\mathbf{r}_1,t) \\ = \; & \frac{1}{2}\int d^4x_1 d^4x_2 \psi_\gamma^\dagger(x_1)\psi_\delta^\dagger(x_2)V_s(x_1-x_2)\psi_\delta(x_2)\psi_\gamma(x_1), \end{aligned} \tag{78}$$

in which $V_s(x_1 - x_2)$ is defined in Eq. (40).

Expand the exponential,

$$e^{-i\int dtV_I} = 1 - \frac{i}{2}\int d^4x_1 d^4x_2 \cdots \tag{79}$$

Then for the numerator of Eq. (77), the first term is,

$$-i\langle\Phi_0|T\psi_\alpha(x)\psi_\beta^\dagger(x')|\Phi_0\rangle = G^0_{\alpha\beta}(x,x'). \tag{80}$$

The second term is of the form,

$$\frac{(-i)^2}{2}\int d^4x_1 d^4x_2 \langle T\psi_1^\dagger\psi_2^\dagger\psi_2\psi_1\psi_x\psi_{x'}^\dagger\rangle V_s(x_1-x_2). \tag{81}$$

There are six ways to contract the field operators (see Fig. 2). In the figure, a segment of a solid line represents a Green function, and a wavy line represents an interaction. The first and the second are *disconnected* diagrams. They'll be cancelled by diagrams in the denominator $\langle -\infty|\infty\rangle$ (more details below).

Following the same procedure, one can show that the denominator generates the following diagrams,

$\langle -\infty|\infty\rangle$ = 1 + $\frac{1}{2}$  + $\frac{1}{2}$  + ... (82)

A. Linked cluster theorem

According to the **linked cluster theorem**, which won't be proven here, only **connected diagrams** contribute to $G_{\alpha\beta}$ (see Sec. 8.3 of Ref. 3). For example, to the first order,

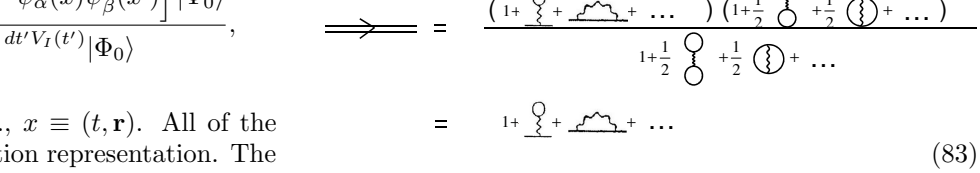

(83)

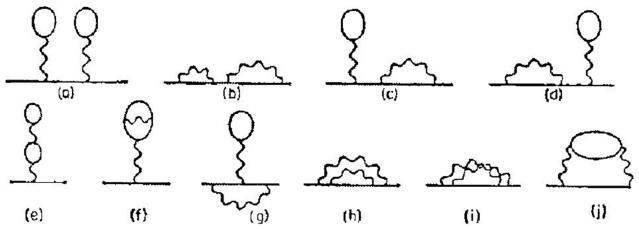

FIG. 4 Connected diagrams at the second order.

This is exact to all orders of expansion! Therefore,

$$G_{\alpha\beta}(x,x') = -i\left\langle Te^{-i\int dt_1 V_I}\psi_\alpha(x)\psi^\dagger_\beta(x')\right\rangle_c . \quad (84)$$

The subscript c means that only connected diagrams are included.

All of the connected diagrams at the first order and the second order are shown in Figs. 3, 4. In Fig. 4, there are two wavy lines in each diagram because of two V_I's in each term. In general, for a n-th order diagram, there are n wavy lines, and $2n+1$ segments of solid lines ($G^0_{\alpha\beta}$'s) due to the contraction of $4n+2$ field operators.

In general,

$$G = G^0 + G^1 + G^2 + \cdots , \quad (85)$$

where

$$G^1 = G^0\Sigma^1 G^0, \quad \Sigma^1 = \text{ 2 types in Fig. 3,} \quad (86)$$
$$G^2 = G^0\Sigma^2 G^0, \quad \Sigma_2 = 10 \text{ types in Fig. 4,} \quad (87)$$
$$\cdots$$

Or,

$$G = G^0 + G^0\Sigma G^0,$$
$$\text{where } \Sigma = \Sigma^1 + \Sigma^2 + \cdots . \quad (88)$$

The Σ's are called **self-energy diagrams**.

B. Dyson equation

Diagrams (a)∼(d) in Fig. 4 can be separated to two parts by cutting only one solid line. We call these *reducible* (or *improper*) self-energy diagrams. Diagrams (e)∼(j) are *irreducible* (or *proper*) because they would not be separated by cutting just one solid line.

Σ^2_{red} can always be written as $\Sigma^1 G^0 \Sigma^1$, similarly for higher orders. In general, if Σ^* represents irreducible, or **proper self-energy**, then

$$\Sigma = \Sigma^* + \Sigma^* G^0 \Sigma^* + \Sigma^* G^0 \Sigma^* G^0 \Sigma^* + \cdots . \quad (89)$$

It follows that,

$$G = G^0 + G^0\Sigma^* G, \quad (90)$$
$$\text{or } G = \frac{1}{(G^0)^{-1} - \Sigma^*}. \quad (91)$$

This is the **Dyson equation**, which can be represented by the diagrams in Fig. 5 (a).

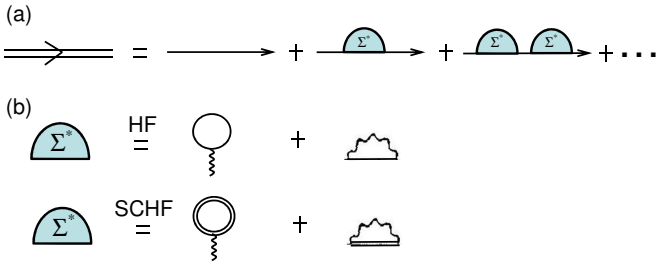

FIG. 5 The Dyson equation in diagrams. (a) Fermion propagator dressed by proper self-energies. (b) The self-energy in (a) that corresponds to the HFA and the self-consistent HFA.

V. GREEN FUNCTION IN MOMENTUM SPACE

For a system with translation symmetry, it is convenient to calculate the Green function in momentum space. Let's start with an electron gas with the Hamiltonian,

$$H = \sum_{k\alpha} \omega_{k\alpha} a^\dagger_{k\alpha} a_{k\alpha} + V_{ee}, \ \alpha = \text{spin}. \quad (92)$$

The Green function is,

$$G_{\alpha\beta}(\mathbf{k}, t-t') = -i\langle\Phi_0|Te^{-i\int dt_1 V_{ee}} a_{k\alpha}(t) a^\dagger_{k\beta}(t')|\Phi_0\rangle_c. \quad (93)$$

In frequency variable, it is

$$G_{\alpha\beta}(\mathbf{k},\omega) = \int_{-\infty}^{\infty} dt e^{i\omega(t-t')} G_{\alpha\beta}(\mathbf{k}, t-t'). \quad (94)$$

The zeroth-order Green function is given in Eq. (17),

$$G^0_{\alpha\beta}(\mathbf{k},\omega) = \delta_{\alpha\beta}\left(\frac{1-n_k}{\omega-\omega_k+i\eta} + \frac{n_k}{\omega-\omega_k-i\eta}\right)$$
$$= \delta_{\alpha\beta} G^0_\alpha(\mathbf{k},\omega). \quad (95)$$

To the first order, we have

$$G_{\alpha\beta}(\mathbf{k},\omega) = G^0_{\alpha\beta}(\mathbf{k},\omega) \quad (96)$$
$$-i\int dt e^{i\omega(t-t')}(-i)\int dt_1 \left\langle TV_{ee}(t_1) a_{k\alpha}(t) a^\dagger_{k\beta}(t')\right\rangle_c ,$$

where

$$V_{ee}(t) = \frac{1}{2V_0}\sum_{k_1 k_2 q}\sum_{\gamma_1\gamma_2\gamma_1'\gamma_2'} \quad (97)$$
$$V^{(2)}_{\gamma_1'\gamma_2'\gamma_2\gamma_1}(\mathbf{q}) a^\dagger_{k_1+q,\gamma_1'}(t) a^\dagger_{k_2-q,\gamma_2'}(t) a_{k_2,\gamma_2}(t) a_{k_1,\gamma_1}(t).$$

If the interaction is spin-independent, then

$$V^{(2)}_{\gamma_1'\gamma_2'\gamma_2\gamma_1}(\mathbf{q}) = V(\mathbf{q})\delta_{\gamma_1'\gamma_1}\delta_{\gamma_2'\gamma_2}. \quad (98)$$

Now, for connected diagrams,

$$\left\langle Ta^\dagger_{\gamma_1'}(t_1) a^\dagger_{\gamma_2'}(t_1) a_{\gamma_2}(t_1) a_{\gamma_1}(t_1) a_\alpha(t) a^\dagger_\beta(t')\right\rangle_c$$
$$= \langle Ta_{\gamma_1}(t_1) a^\dagger_\beta(t')\rangle\langle Ta^\dagger_{\gamma_1'}(t_1) a_{\gamma_2}(t_1)\rangle\langle Ta^\dagger_{\gamma_2'}(t_1) a_\alpha(t)\rangle$$
$$- \langle Ta_{\gamma_1}(t_1) a^\dagger_\beta(t')\rangle\langle Ta^\dagger_{\gamma_2'}(t_1) a_{\gamma_2}(t_1)\rangle\langle Ta^\dagger_{\gamma_1'}(t_1) a_\alpha(t)\rangle$$
$$+ \text{ another 2 terms with } (\gamma_1 \leftrightarrow \gamma_2). \quad (99)$$

Therefore, using Eq. (74), we have

$$\begin{aligned}
&(-i)^3\langle T\cdots\rangle_c \\
=\ & G^0_{\gamma_1\beta}(\mathbf{k},t_1-t')G^0_{\gamma_2\gamma_1'}(\mathbf{k}_2,0^-)G^0_{\alpha\gamma_2'}(\mathbf{k},t-t_1) \\
& \times\delta_{kk_1}\delta_{k_1+q,k_2}\delta_{k_2-q,k} \\
-\ & G^0_{\gamma_1\beta}(\mathbf{k},t_1-t')G^0_{\gamma_2\gamma_2'}(\mathbf{k}_2,0^-)G^0_{\alpha\gamma_1'}(\mathbf{k},t-t_1) \\
& \times\delta_{kk_1}\delta_{k_2-q,k_2}\delta_{k_1+q,k} \\
+\ & \text{another 2 terms with } (\gamma_1\leftrightarrow\gamma_2). \qquad (100)
\end{aligned}$$

Note that,

$$\begin{aligned}
G^0_{\gamma_2\gamma_1'}(\mathbf{k}_2,0^-) &= -i\langle Ta_{\gamma_2}(0)a^\dagger_{\gamma_1'}(0^+)\rangle \qquad (101)\\
&= i\langle a^\dagger_{\gamma_1'}(0^+)a_{\gamma_2}(0)\rangle. \qquad (102)
\end{aligned}$$

Also, $e^{i\omega(t-t')}=e^{i\omega(t-t_1)}e^{i\omega(t_1-t')}$. Therefore,

$$\begin{aligned}
&G^1_{\alpha\beta}(\mathbf{k},\omega) \\
=\ & \frac{(-i)^2}{2V_0}\sum_{k_1k_2q}\sum_{\gamma_1\gamma_2\gamma_1'\gamma_2'}\int dtdt_1e^{i\omega(t-t')}V^{(2)}_{\gamma_1'\gamma_2'\gamma_2\gamma_1}(\mathbf{q})\langle T\cdots\rangle_c \\
=\ & \frac{i}{V_0}\sum_{q\gamma_2}V^{(2)}_{\gamma_2\alpha\gamma_2\beta}(\mathbf{q})G^0_\beta(\mathbf{k},\omega)G^0_{\gamma_2}(\mathbf{k}+\mathbf{q},0^-)G^0_\alpha(\mathbf{k},\omega) \\
-\ & \frac{i}{V_0}\sum_{k_2\gamma_2}V^{(2)}_{\alpha\gamma_2\gamma_2\beta}(0)G^0_\beta(\mathbf{k},\omega)G^0_{\gamma_2}(\mathbf{k}_2,0^-)G^0_\alpha(\mathbf{k},\omega)
\end{aligned}$$

=

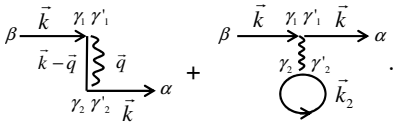

Note that the internal variables of a diagram needs be summed, and

$$G^0_{\gamma_2}(\mathbf{k}_2,0^-)=\int\frac{d\omega'}{2\pi}G^0_{\gamma_2}(\mathbf{k}_2,\omega')\underbrace{e^{-i\omega'0^-}}_{e^{i\omega'\eta},\ \eta>0}. \qquad (103)$$

For spin-independent interaction, we have

$$\begin{aligned}
\sum_\gamma V^{(2)}_{\gamma\alpha\gamma\beta}(\mathbf{q}) &= V(\mathbf{q})\delta_{\alpha\beta}, \qquad (104)\\
\sum_\gamma V^{(2)}_{\alpha\gamma\gamma\beta}(\mathbf{q}) &= 2V(\mathbf{q})\delta_{\alpha\beta}. \qquad (105)
\end{aligned}$$

Also, for the instantaneous potential,

$$V_s(q)=\int dxV_s(x)e^{iqx}=V(\mathbf{q}), \qquad (106)$$

in which q,x are 4-vectors, $q=(q_0,\mathbf{q})$ or $(\omega,\mathbf{q})$, and $qx\equiv\omega t-\mathbf{q}\cdot\mathbf{r}$.

Use

$$\frac{1}{V_0}\sum_{\mathbf{q}}\int\frac{d\omega}{2\pi}\to\int\frac{d^4q}{(2\pi)^4}, \qquad (107)$$

shift $\mathbf{q}$ to $\mathbf{q}-\mathbf{k}$, also $V(-\mathbf{q}=V(\mathbf{q}))$, it follows that,

$$\begin{aligned}
G^1_{\alpha\beta}(k) &= G^0_\beta(k)\Bigg[\underbrace{-2i\int\frac{d^4q}{(2\pi)^4}V_s(0)G^0_\alpha(q)e^{iq_0\eta}}_{\text{Hartree}} \qquad (108)\\
&\quad+\underbrace{i\int\frac{d^4q}{(2\pi)^4}V_s(k-q)G^0_\alpha(q)e^{iq_0\eta}}_{\text{Fock}}\Bigg]G^0_\alpha(k)\delta_{\alpha\beta}.
\end{aligned}$$

The self-energies inside the square bracket are shown in Fig. 5 (b). If the nude G^0 is replaced by the dressed G, then we have the **self-consistent Hartree-Fock approximation**.

In the first term, we have

$$\begin{aligned}
&\int\frac{d^4q}{(2\pi)^4}G^0_\alpha(q)e^{iq_0\eta} \\
=\ & \int\frac{d^3\mathbf{q}}{(2\pi)^3}\frac{dq_0}{2\pi}\left(\frac{1-n_q}{q_0-\omega_q+i\delta}+\frac{n_q}{q_0-\omega_q-i\delta}\right)e^{iq_0\eta} \\
=\ & i\int\frac{d^3\mathbf{q}}{(2\pi)^3}n_q \\
=\ & i\frac{N/2}{V_0}, \quad 2 \text{ due to spin.} \qquad (109)
\end{aligned}$$

Because of the factor $e^{iq_0\eta}$, we have to close the path of the q_0-integral over the upper-half complex plane (see Fig. 1). The time integral in the second term can be handled similarly. Finally, the HF self-energy is,

$$\Sigma^1(k)=\underbrace{V(0)\frac{N}{V_0}}_{\text{Hartree}}-\underbrace{\int\frac{d^3\mathbf{q}}{(2\pi)^3}V(\mathbf{k}-\mathbf{q})n_q}_{\text{Fock}}. \qquad (110)$$

To the first order,

$$G_\alpha(\mathbf{k},\omega)=\frac{1}{(G^0_\alpha)^{-1}-\Sigma^1_k}=\frac{1}{\omega-\omega_k-\Sigma^1_k}. \qquad (111)$$

The pole of one-particle Green function, $\omega=\omega_k+\Sigma^1_k$, determines the energy of a **quasi-particle**. In the next chapter, we'll see that the pole of two-particle Green function determines the energy dispersion of **collective excitation**.

A. Feynman rules

For the diagrams in momentum space, we have the following rules for electron self-energy.
1. At the n-th order, draw all topologically distinct connected diagrams with n wavy lines and $2n+1$ solid lines.
2. Each solid line is $G^0_{\alpha\beta}(k)$. For a closed loop, or a segment linked by the same wavy line, alter it to $G^0_{\alpha\beta}(k)e^{ik_0\eta}$ (see Eq. 102).

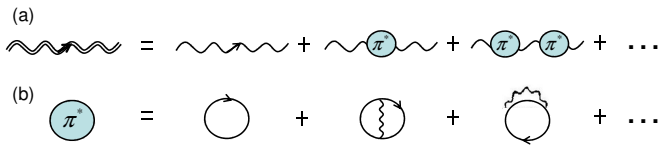

FIG. 6 (a) Interaction line dressed by self-energies. (b) Low-order terms in self-energy.

3. Each wavy line is $V_{\gamma_1'\gamma_2'\gamma_2\gamma_1}(q)$.
4. Associate each line with a 4-momentum, and the 4-momentum flow needs be conserved at each vertex.
5. Sum over internal degrees of freedom (4-momentum, spin ... etc), $(1/V_0)\sum_{k\alpha\cdots}$.
6. Multiply the summation by $i^n(-1)^F$, where n is the order (or half of the number of vertices), and F is the number of closed fermion loops. Note: for photon self-energy, n is one-half of the number of vertices (or the number of internal momenta). See Ref. 3.

For example, for spin-independent bare-particle energy $\omega_{k\alpha}\to\omega_k$, $G^0_\alpha\to G^0$, and spin-independent interaction,

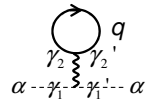

$$= -i\sum_{\gamma_2\gamma_2'}\int\frac{d^4q}{(2\pi)^4}G^0_{\gamma_2\gamma_2'}(q)e^{iq_0\eta}V^{(2)}_{\alpha\gamma_2'\gamma_2\alpha}(0)$$
$$= -\underbrace{2}_{\text{spin}}i\int\frac{d^4q}{(2\pi)^4}G^0(q)e^{iq_0\eta}V_s(0), \quad (112)$$

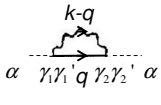

$$= i\sum_{\gamma_1'\gamma_2}\int\frac{d^4q}{(2\pi)^4}G^0_{\gamma_1'\gamma_2}(q)e^{iq_0\eta}V_{\gamma_1'\alpha\gamma_2\alpha}(k-q)$$
$$= i\int\frac{d^4q}{(2\pi)^4}G^0(q)e^{iq_0\eta}V_s(k-q). \quad (113)$$

These are the two terms in Eq. (108).

As another example, consider the **bubble diagram** in photon self-energy. According to the Feynman rules,

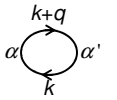

$$= -i\sum_{\alpha\alpha'}\int\frac{d^4k}{(2\pi)^4}G^0_{\alpha\alpha'}(k)G^0_{\alpha'\alpha}(k+q) \quad (114)$$
$$= -2i\int\frac{d^4k}{(2\pi)^4}G^0(k)G^0(k+q)\equiv\Pi_0(q).$$

This is the lowest order term in the self-energy of interaction line (see Fig. 6). In general,

$$V_{eff}(q) = V_s(q)+V_s(q)\Pi^*(q)V_s(q)+\cdots$$
$$= \frac{V_s(q)}{1-\Pi^*(q)V_s(q)}=\frac{V(\mathbf{q})}{\epsilon(q)}, \quad (115)$$
$$\text{where } \epsilon(q) = 1-\Pi^*(q)V(\mathbf{q}). \quad (116)$$

The Π^* in Eq. (114) is essentially the density response function χ^0_ρ in Chap 3 (see Prob 3). In the next Sec, we study the polarization due to the bubble diagram. This is also known as the **random phase approximation**, because it's equivalent to the "random phase" (literally) approximation in the EOM approach by Bohm, Pines, and Sawada (see Sec 4.3 of Ref. 4). This is a good approximation if the electron density is high, $k_Fa_0\gg 1$. For low-density electron gas, ladder diagrams would be more important. See Chap 10 of Ref. 6 for more details.

VI. ELECTRIC POLARIZATION

Recall that G^0 is given in Eq. (95). Thus,

$$\Pi_0(q) = -2i\int\frac{d^4k}{(2\pi)^4}G^0(k)G^0(k+q) \quad (117)$$
$$= -2i\int\frac{d^3kdk_0}{(2\pi)^4}\left(\underbrace{\frac{1-n_k}{k_0-\omega_k+i\eta}}_{\text{poles at LHP}}+\underbrace{\frac{n_k}{k_0-\omega_k-i\eta}}_{\text{poles at UHP}}\right)$$
$$\times\left(\underbrace{\frac{1-n_{k+q}}{k_0+q_0-\omega_{k+q}+i\eta}}_{\text{poles at LHP}}+\underbrace{\frac{n_{k+q}}{k_0+q_0-\omega_{k+q}-i\eta}}_{\text{poles at UHP}}\right).$$

After the multiplication, there are four terms in the integrand. For the LHP×LHP (UHP×UHP) term, if we choose the path of integration to be an infinite half-circle over the upper-half (lower-half) plane, then the result is zero since no pole is enclosed. That is, only cross terms survive. Using the **Cauchy residue theorem**,

$$\oint_c dz\frac{f(z)}{z-z_0}=2\pi i f(z_0), \quad (118)$$

we can get

$$\Pi_0(q) = 2\int\frac{d^3k}{(2\pi)^3}\left[\frac{n_k(1-n_{k+q})}{q_0+\omega_k-\omega_{k+q}+2i\eta}\right.$$
$$\left.+\frac{(1-n_k)n_{k+q}}{q_0+\omega_k-\omega_{k+q}-2i\eta}\right] \quad (119)$$
$$= 2\int\frac{d^3k}{(2\pi)^3}\left(\frac{n_k-n_kn_{k+q}}{q_0-\omega_{kq}+2i\eta}+\frac{n_kn_{k+q}-n_{k+q}}{q_0-\omega_{kq}-2i\eta}\right),$$

where

$$\omega_{kq}\equiv\omega_{k+q}-\omega_k=\frac{1}{2m}(2\mathbf{k}\cdot\mathbf{q}+q^2). \quad (120)$$

For its retarded counterpart, flip the sign of $-2i\eta$ in the second term, and get

$$\Pi^R_0(q)=2\int\frac{d^3k}{(2\pi)^3}\frac{n_k-n_{k+q}}{q_0-\omega_{kq}+2i\eta}. \quad (121)$$

This agrees with the χ^0_ρ in Chap 3.

Use the Plemelj formula,

$$\lim_{\eta\to0}\frac{1}{x\pm i\eta}=P\frac{1}{x}\mp i\pi\delta(x), \quad (122)$$

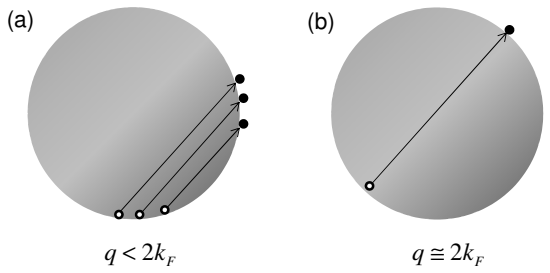

FIG. 7 Creation of an electron-hole pair when (a) $q < 2k_F$, and (b) $q \simeq 2k_F$.

then one has,

$$\begin{aligned} \text{Re } \Pi_0(q) &= 2P \int \frac{d^3k}{(2\pi)^3} \frac{n_k - n_{k+q}}{q_0 + \omega_k - \omega_{k+q}} \qquad (123) \\ \text{or} &= 2P \int \frac{d^3k}{(2\pi)^3} n_k \left(\frac{1}{q_0 - \omega_{kq}} - \frac{1}{q_0 + \omega_{kq}} \right). \end{aligned}$$

We have changed $\mathbf{k} + \mathbf{q} \to -\mathbf{k}$ to get the second expression, which only involves filled states. For the imaginary part,

$$\text{Im } \Pi_0(q) = -2\pi \int \frac{d^3k}{(2\pi)^3} n_k (1 - n_{k+q}) \delta(q_0 - \omega_{kq}). \quad (124)$$

We have dropped the second delta function, assuming $q_0 > 0$ (the factor $n_k(1 - n_{k+q})$ ensures that $\omega_{kq} > 0$). This is proportional to the absorption probability converting a photon to an e-h pair. For more discussion, see p. 159 of Ref. 2.

A. Static polarization

For the static case, $q_0 = 0$, and

$$\text{Im } \Pi_0(\mathbf{q}, 0) = 0. \qquad (125)$$

Thus (see Sec. 14 of Ref.2),

$$\begin{aligned} \Pi_0(\mathbf{q}, 0) &= -2 \int \frac{d^3k}{(2\pi)^3} n_k \frac{2}{\omega_{k+q} - \omega_k} \qquad (126) \\ &= -D(\varepsilon_F) \underbrace{\left(\frac{1}{2} + \frac{1 - x^2}{4x} \ln \frac{1 + x}{1 - x} \right)}_{F_L(x),\ \text{Lindhard function}} < 0 \end{aligned}$$

where $D(\varepsilon_F) = mk_F/\hbar^2\pi^2$, and $x = q/2k_F$. This reproduces the result in Sec. II.C.1 of Chap 3.

The derivative of the Lindhard function has a singularity at $q = 2k_F$ (see Chap 2). This is related to the following fact: The integrand in Eq. (123) has the numerator $n_{k+q} - n_k$, which is non-zero when $\varepsilon_k < \varepsilon_F$ and $\varepsilon_{k+q} > \varepsilon_F$. This corresponds to the creation of an electron-hole (e-h) pair with momentum $\mathbf{q}$ (see Fig. 7). The phase space available for such a process drops suddenly when $q = 2k_F$.

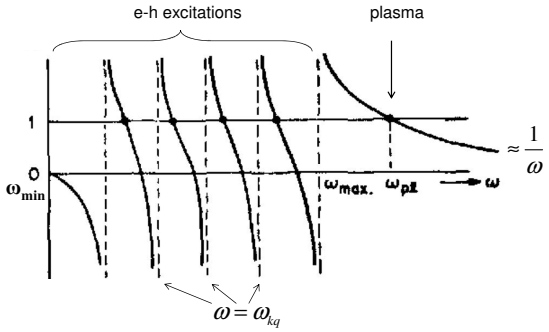

FIG. 8 Graphic solutions of Eq. (128). The curves are plotted using the LHS of the equation. At high frequency, it approaches $1/\omega$.

As mentioned in Chap 3, such a singularity leads to the Friedel oscillation of electron density. It is also responsible for the **Kohn anomaly** in phonon spectrum. In 1D, electron-hole pairs with $q \simeq 2k_F$ dominate low-energy excitations, which makes the singularity more severe. It would cause spontaneous lattice dimerization in a half-filled energy band. This is called the **Peierls instability**.
Note: In 2D, the singular behavior at $q = 2k_F$ could be enhanced by the **nesting** of Fermi surface.

B. Dynamic polarization

To the lowest order,

$$V_{eff}(q) = \frac{V(\mathbf{q})}{1 - \Pi_0(q) V(\mathbf{q})}. \qquad (127)$$

If $\Pi_0(q)V(\mathbf{q}) = 1$, then the dielectric function $\epsilon(\mathbf{q}, \omega) = 0$, and there exists elementary excitations in the electron gas. Consider the real part,

$$\text{Re } \Pi_0(q) = 2 \int \frac{d^3k}{(2\pi)^3} \frac{n_k - n_{k+q}}{q_0 - \omega_{kq}}.$$

To meet the condition $\Pi_0 V = 1$, one needs (adopt finite-space version, and rewrite q_0 as ω)

$$V(\mathbf{q}) \frac{2}{V_0} \sum_k \frac{n_k - n_{k+q}}{\omega - \omega_{kq}} = 1. \qquad (128)$$

The excitation energy of an e-h pair (neglecting interaction) is bounded,

$$\frac{1}{2m}(q^2 - 2k_F q) \le \omega_{kq} \le \frac{1}{2m}(q^2 + 2k_F q). \qquad (129)$$

The denominator of Eq. (128) can be zero when ω falls within this range. The left hand side of Eq. (128) as a function of frequency is plotted in Fig. 8. This equation has solutions when the curves intersect with the horizontal line at height 1.

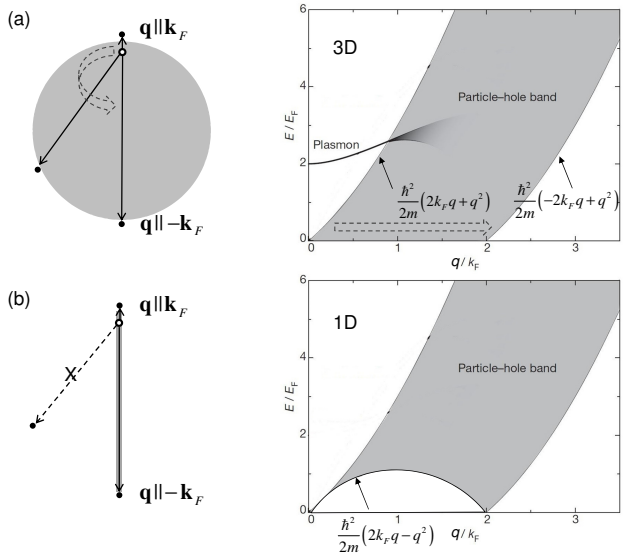

FIG. 9 Elementary excitations of an electron gas in (a) 3D and (b) 1D . The figures on the left are low-energy e-h pair excitations near the surfaces of Fermi spheres. The excitations in 2D are similar to those in 3D, except that the plasma excitation is gapless.

There are two types of excitations: (1) Those in the range $\omega_{min} \le \omega \le \omega_{max}$ are e-h excitations (quasiparticles). (2) The one with $\omega > \omega_{max}$ is a plasma wave (collective excitation), which can be viewed as a coherent e-h excitation. For an infinite system with $V_0 \to \infty$, the e-h excitations are dense in energy (see Fig. 9 (a)).

Note that when $\omega = \omega_{kq}$, the imaginary part Im $\Pi_0(\mathbf{q}) \neq 0$. As a result, the e-h pair has a finite lifetime. This is called **Landau damping**.

In 1D, there is a blank area at low energy in Fig. 9 (b), in which e-h excitations are forbidden. This is due to the fact that in 1D, the momentum $\mathbf{q}$ of an e-h pair can only be parallel or anti-parallel to $\mathbf{k}_F$ (see the plot on the left).

To get the energy dispersion of the plasma wave, let $|\mathbf{q}| \to 0$, and use

$$n_{k+q} - n_k \simeq \omega_{kq} \frac{\partial n_k}{\partial \omega_k}, \tag{130}$$

then

$$\begin{aligned} & \frac{2}{V_0} \sum_k \frac{n_k - n_{k+q}}{\omega - \omega_{kq}} \\ \simeq\ & \frac{2}{V_0} \sum_k \left(-\frac{\partial n_k}{\partial \omega_k} \right) \frac{\omega_{kq}}{\omega - \omega_{kq}} \\ =\ & \frac{1}{2\pi^2} \int k^2 dk \delta(\omega_k - \varepsilon_F) \int_{-1}^{1} d\cos\theta \frac{(kq/m)\cos\theta}{\omega - (kq/m)\cos\theta} \\ \cdots\ & \text{(see p. 261 of Bruus and Flensberg)} \\ =\ & \underbrace{\frac{k_F^3}{3\pi^2}}_{n} \frac{q^2}{m\omega^2} \left[1 + \frac{3}{5} \left(\frac{qv_F}{\omega} \right)^2 + \cdots \right]. \end{aligned} \tag{131}$$

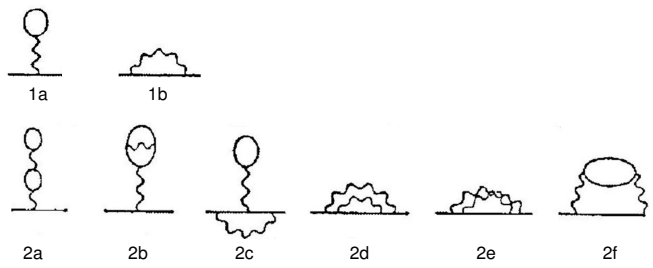

FIG. 10 Irreducible self-energies of an electron at the first order and the second order.

Recall that $V(\mathbf{q}) = 4\pi e^2/q^2$. It can be shown that the resonant condition gives,

$$\omega^2 = \underbrace{\frac{4\pi n e^2}{m}}_{\omega_p^2} + \frac{6\varepsilon_F}{5} \frac{q^2}{m} + \cdots, \tag{132}$$

or

$$\omega(q) = \omega_p + \alpha \frac{q^2}{m}, \quad \alpha = \frac{3\varepsilon_F}{5\omega_p} = \frac{0.64}{\sqrt{r_s}}. \tag{133}$$

This is the same as the result in Chap 3.

VII. VERTEX CORRECTION

In Fig. 10, we have listed again the irreducible self-energy diagrams up to the second order of interaction. For reference, there is no reducible self-energy at the first order (see Fig. 4), but four reducible self-energies at the second order. At the third order, there are 74 self-energy diagrams: 32 reducible, and 42 irreducible. See Ref. 5 for a complete list if you're curious.

If we use dressed particle line and dressed interaction line below,

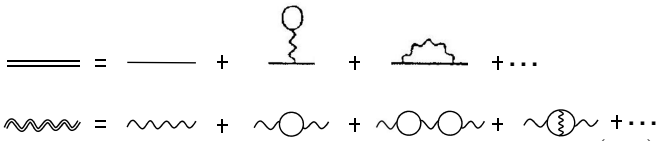

(134)

then except (2e), all of the figures in Fig. 10 belong to the following **skeleton diagrams**.

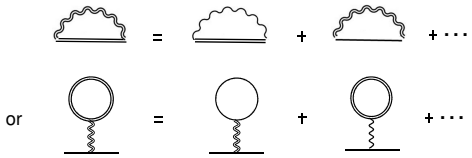

(135)

Obviously, a diagram with two external particle lines or two external interaction lines can be included in a dressed solid or wavy line. However, a diagram with two external particle lines and one external interaction line might not

be. Some examples of such diagrams are,

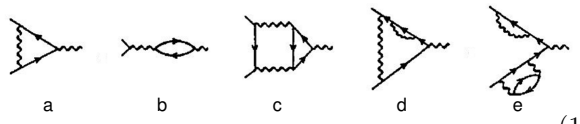

(136)

These **vertex diagrams** can be divided into two types: It is called a reducible vertex if, by cutting one solid line or one wavy line, the diagram is disconnected. For example, diagrams (b) and (e) are reducible, while (a), (c), (d) are irreducible.

Reducible vertices can be simplified by replacing external lines with dressed lines, and thus belong to the two skeleton diagrams above. On the other hand, irreducible (or proper) vertices cannot be simplified this way. Those cannot be lumped to the two sets above can be collected as,

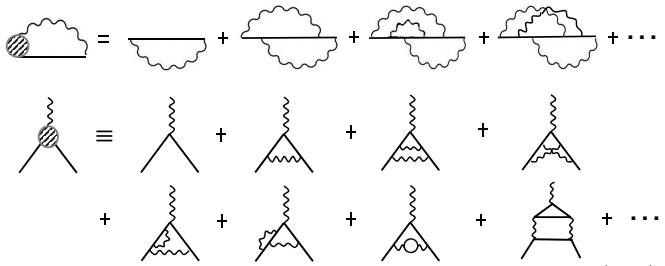

(137)

The blob is called a **vertex correction**.

Note that there is no vertex correction to  , since

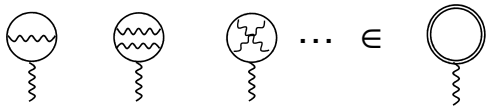

(138)

Thus, finally

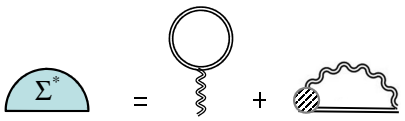

(139)

For more details, see Chap 11 of Ref. 6.

When you calculate the electrical conductivity, vertex correction for diagrams dealing with impurities needs be considered to get the correct **transport relaxation time**, otherwise the **quasi-particle relaxation time** is obtained instead (Ref. 7, also Chap 8).

Exercise:

1. The non-interacting Green function in the frequency domain is written as

$$G^0_{\alpha\beta}(\omega) = \left(\frac{1-n_\alpha}{\omega-\omega_\alpha+i\eta} + \frac{n_\alpha}{\omega-\omega_\alpha-i\eta}\right)\delta_{\alpha\beta}.$$

By Fourier-transforming $G^0_{\alpha\beta}(\omega)$, show that

$$G^0_{\alpha\beta}(t-t') = e^{-i\omega_\alpha t}\left[-i\theta(t-t')(1-n_\alpha) + i\theta(t'-t)n_\alpha\right]\delta_{\alpha\beta},$$

where $\theta(t-t')$ is the step function.

2. In general, the Green function for interacting electrons can be written as

$$G(k) = \frac{1}{\omega - \varepsilon^0_{\mathbf{k}} - \Sigma(k)}, \tag{140}$$

where $k = (\mathbf{k}, \omega)$. The proper self-energy may have both real and imaginary parts, $\Sigma = \Sigma' + i\Sigma''$. Define the quasi-particle energy as $\varepsilon(k) = \varepsilon^0_{\mathbf{k}} + \Sigma'(k)$, and let $\varepsilon(\mathbf{k}_F, 0) = 0$ (this defines $\mathbf{k}_F$). Taylor-expand $\varepsilon(k)$ to first order around $(\mathbf{k}_F, 0)$ and show that

$$G(k) \simeq \frac{Z}{\omega - \tilde{\varepsilon}_{\mathbf{k}} - iZ\Sigma''}, \tag{141}$$

where

$$Z^{-1} = 1 - \frac{\partial\Sigma'(\mathbf{k}_F, 0)}{\partial\omega}, \tag{142}$$

$$\tilde{\varepsilon}_{\mathbf{k}} = Z(\mathbf{k}-\mathbf{k}_F)\cdot\frac{\partial}{\partial\mathbf{k}_F}\mathrm{Re}\ \varepsilon(\mathbf{k}, 0). \tag{143}$$

3. The time-ordered density response function for a homogeneous system is given as,

$$\chi^T_{\rho\rho}(\mathbf{k},\omega) = -\frac{i}{V_0}\int dt e^{i\omega t}\langle\Psi_0|T\rho(\mathbf{k},t)\rho(-\mathbf{k},0)|\Psi_0\rangle, \tag{144}$$

where $|\Psi_0\rangle$ is the many-body ground state.

(a) For an interacting electron gas, show that,

$$\langle\Psi_0|T\rho(\mathbf{k},t)\rho(-\mathbf{k},0)|\Psi_0\rangle = \langle\Phi_0|Te^{-i\int dt_1 V_{ee}}\rho(\mathbf{k},t)\rho(-\mathbf{k},0)|\Phi_0\rangle_c$$

where $|\Phi_0\rangle$ is the non-interacting ground state.

(b) Expand to the "zero-th order" in V_{ee}, show that $\chi^{T,0}_{\rho\rho}(\mathbf{k},\omega)$ corresponds to the bubble diagram in RPA.

4. Two metal leads, A and B, are held at different chemical potentials, μ_A and $\mu_B = \mu_A + e\Delta V$. The leads are separated by a thin slab of insulator. The electrons in one lead can tunnel through the insulator to the other lead via the coupling,

$$H_T = \sum_{\alpha\beta}\left(t_{\alpha\beta}a^\dagger_\alpha b_\beta + t^*_{\alpha\beta}b^\dagger_\beta a_\alpha\right), \tag{145}$$

where $a^\dagger_\alpha$ ($b^\dagger_\beta$) creates an electron in lead A(B). The transition rate of tunnelling from B to A is given by the Fermi Golden rule,

$$W_{\beta\to\alpha} = 2\pi\sum_F |\langle F|t_{\alpha\beta}a^\dagger_\alpha b_\beta|I\rangle|^2\delta(E_F - E_I), \tag{146}$$

where the initial states and the final states are

$$|I\rangle = |\psi^{N_A}_0\rangle|\psi^{N_B}_0\rangle,$$
$$|F\rangle = |\psi^{N_A+1}_{n_A}\rangle|\psi^{N_B-1}_{n_B}\rangle, \tag{147}$$

$\sum_F = \sum_{n_A n_B}$, and

$$E_F - E_I = E^{N_A+1}_{n_A} + E^{N_B-1}_{n_B} - E^{N_A}_0 - E^{N_B}_0 = \omega_{n_A 0} + \omega_{n_B 0}, \tag{148}$$

where $\omega_{n_A 0} \equiv E_{n_A}^{N_A+1} - E_0^{N_A}$, and $\omega_{n_B 0} \equiv E_{n_B}^{N_B-1} - E_0^{N_B}$.
(a) With the help of

$$\delta(E_F - E_I) = \int d\omega \delta(\omega - \omega_{n_A 0}) \delta(\omega + \omega_{n_B 0}), \quad (149)$$

show that

$$W_{\beta\to\alpha} = 2\pi |t_{\alpha\beta}|^2 \int_0^\infty d\omega A_\alpha^+(\omega) A_\beta^-(\omega - e\Delta V), \quad (150)$$

in which the spectral functions are given by

$$\begin{aligned} A_\alpha^+(\omega) &= \sum_{n_A} |\langle \psi_{n_A}^{N_A+1} | a_\alpha^\dagger | \psi_0^{N_A} \rangle|^2 \delta(\omega - \omega_{n_A 0}), \\ A_\beta^-(\omega) &= \sum_{n_B} |\langle \psi_{n_B}^{N_B-1} | b_\beta | \psi_0^{N_B} \rangle|^2 \delta(\omega + \omega_{n_B 0}). \end{aligned} \quad (151)$$

(b) Even though $W_{\beta\to\alpha}$ is integrated over all $\omega > 0$, the integrand is nonzero only over a finite interval of energies. What are the lower bound and upper bound of this interval?
Ref: Sec. 8.4 of Ref. 2.

References

[1] Quantum Theory of the Electron Liquid, by Gabriele F. Giuliani and Giovanni Vignale, Cambridge University Press, 2005.
[2] A.L. Fetter, J.D. Walecka, Quantum Theory of Many-Particle Systems, Dover Books, 2003.
[3] Methods of Quantum Field Theory in Statistical Physics, by A. A. Abrikosov, L. P. Gorkov, and I. E. Dzyaloshinski, Dover Publications, 1975.
[4] Green function theory in quantum statistics (in Chinese), by C. H. Tsai and others, 1982.
[5] R. J. Mathar, Int J Quantum Chem, **107** 1975 (2007).
[6] A guide to Feynman diagrams in the many-body problem, 2nd ed., by R. D. Mattuck, Dover Publication, 1976.
[7] S. Das Sarma and F. Stern, Phys Rev. B **32**, 8442 (1985).